Available online at www.sciencedirect.com
ScienceDirect
International Journal of Heat and Mass Transfer 50 (2007) 2996–3006
International Journal of HEAT and MASS TRANSFER
www.elsevier.com/locate/ijhmt

Optimal conduction pathways for cooling a heat-generating body: A comparison exercise

François Mathieu-Potvin, Louis Gosselin *

Département de génie mécanique, Université Laval, Québec, Que., Canada G1K 7P4

Received 17 August 2006; received in revised form 1 December 2006
Available online 27 March 2007

Abstract

The objectives of this paper are two: (i) propose an evolutionary algorithm for optimizing the topology of a heat-generating area cooled by a high thermal conductivity material in contact with a heat sink, and (ii) compare the evolutionary procedure and optimal structures found to the ones predicted by constructal theory. The evolutionary algorithm starts with an initial random topology, for which control volumes are repositioned based on temperature and heat flux information in order to minimize the hot spot temperature. Significant diminution of the hot spot temperatures have been achieved by the algorithm. Results revealed three families of geometrical configurations for the optimal conductive pathways generated by our algorithm, depending on the values of the conductivity ratio and amount of high thermal conductivity material: few radial blades growing on the heat sink, tree-shaped networks, and networks with loops. The optimal structures are compared with the heat tree architectures generated by constructal theory, and several similarities in terms of performances and geometries are revealed.

Keywords: Conduction; Evolutionary algorithms; Constructal; Topology optimization; Cooling of electronics

1. Introduction

As the lengthscales in engineering continue to diminish, the heat transfer rate density (i.e., the power dissipated per unit of volume or surface) is continuously increasing [1]. One of the most important limitations to the miniaturization and speed of electronic components is their thermal control. Thermal management is crucial in many other systems such as electromagnets, superconductors, motors, lubrication, turbines, buildings, living tissues, etc. The challenge in each case is to package, arrange, and distribute at best the heat-generating elements and cooling pathways within the volume of the system.

In conduction heat transfer, this translates into the fundamental question of how to distribute a finite amount of high thermal conductivity material over a heat-generating surface (or volume) for cooling purpose. In a creative 1997 paper [2], Bejan proposed the constructal approach: an elementary rectangular heat-generating surface with a central highly conductive blade in contact with a cold reservoir is first optimized. The optimal elementary area is then used as a building block, and many of them are assembled on each side of another high conductivity blade to form the first construct. Similarly, several first constructs can be assembled to generate a second construct, and so on [3]. The result is the emergence of a multiscale architecture optimized at each level of construct. Numerical validation of the analysis has been realized in [4]. The shape optimization of the conductive blades [4,5] and of the heat-generating surfaces [6] have been investigated. Later, the constructal approach has been used with triangular [7] and "pizza-slice" elements [8,9]. It has also been used at nanoscale when the conductivity is affected by the size [10].

Another approach to answer the problem of optimal material distribution is to let the entire system morph and change its shape and structure freely, and generate in the

* Corresponding author. Tel.: +1 418 656 7829; fax: +1 418 656 7415.
E-mail address: Louis.Gosselin@gmc.ulaval.ca (L. Gosselin).

0017-9310/$ - see front matter © 2007 Published by Elsevier Ltd.
doi:10.1016/j.ijheatmasstransfer.2006.12.020

Nomenclature

A	area, m^2
d_f	fractal dimension
D	thickness, m
D_i	distance between a heat-generating cell 'i' and its nearest conductive cell, m
$\overline{D}$	averaged $\widetilde{D}_i$
H	height, m
k	thermal conductivity, $W\,m^{-1}\,K^{-1}$
L	length, m
n	number of elemental areas
q'''	volumetric heat generation, $W\,m^{-3}$
R_i	distance between a conductive cell 'i' and the heat sink, m
$\overline{R}$	averaged $\widetilde{R}_i$
T	temperature, K
x,y	cartesian coordinates, m

Greek symbols

ϕ	ratio of the volume occupied by the conductive material

Subscripts

m	minimized quantity
max	maximum value
opt	optimized quantity
p	highly conductive material

Superscript

$\sim$	dimensionless quantity

end the optimal configuration with the use of appropriate algorithms. Due to the large number of possible configurations, heuristic methods such as evolutionary topology optimization algorithms need to be considered. In the past, these approaches have been used in other fields (e.g., strength of materials), but their application to heat transfer system is relatively new. Evolutionary structural optimization has been applied to generate the shape of a one-material surface by eliminating progressively excess elements with heat flux smaller than a certain fraction of the maximal flux value in the domain [11]. In [12], the same authors extended their method to other problems (e.g., incompressible flow, electrostatic) for obtaining uniform fields (e.g., temperature, velocity, electric field) within the domain, either by eliminating step-by-step the useless elements, or by moving these elements. A sensitivity analysis is proposed in Ref. [13] for identifying elements to eliminate (the initial design has an excess of material), in order to reduce the temperature of the system. Heat evacuation was maximized with a finite volume sensitivity analysis in [14] by varying gradually and independently the thermal conductivity of each element. In Ref. [15], the shape of a solid medium embedding heat generating elements was allowed to morph progressively to obtain a desired outer surface temperature with the help of a conjugated gradient algorithm. To weigh up the efficiency of a topological derivative algorithm based on sensitivity analysis, the geometry of a thermal conductive material was smoothly altered by adding holes in the domain of a steady-state heat conduction problem in [16]. To enhance transient heat release from periodically working electronic devices, high conductive cells are distributed through a phase change material by using the integrated temperature gradient over time as a criterion [17].

The objectives of this paper are two: (i) propose an evolutionary algorithm for optimizing the topology of a heat-generating area cooled by a high thermal conductivity material in contact with a heat sink, and (ii) compare the evolutionary procedure and optimal structures found to the ones predicted by constructal theory. The first sections of the paper are describing the evolutionary algorithm and the resulting designs achieved by this procedure. After a brief review of constructal heat trees features, the last sections are dedicated to comparing constructal heat trees to the designs found by the evolutionary algorithm.

2. Problem statement

The problem that we examine in this paper is how to distribute a finite amount of high thermal conductivity material (k_p) on a heat-generating surface of conductivity $k_0 \ll k_p$. The cooling is provided by one or many heat sinks located on the boundary of the heat-generating surface. We assume that the total surface A of the system is fixed. However, the shape of the area is free to vary. The amount of high thermal conductivity material is also fixed, and ϕ is the ratio of the area A occupied by the high thermal conductivity material. This problem formulation corresponds to the one presented in Refs. [2,3].

The dimensionless conduction equation is

$$\frac{\partial}{\partial \tilde{x}}\left(\tilde{k}\frac{\partial \widetilde{T}}{\partial \tilde{x}}\right)+\frac{\partial}{\partial \tilde{y}}\left(\tilde{k}\frac{\partial \widetilde{T}}{\partial \tilde{y}}\right)=-1 \tag{1}$$

where

$$\widetilde{T}=\frac{T-T_0}{q'''A/k_0},\quad \tilde{x},\tilde{y}=\frac{x,y}{A^{1/2}},\quad \tilde{k}=\frac{k}{k_0} \tag{2}$$

The temperature T_0 is the temperature of the cold reservoir, i.e., the heat sink on the boundary of the system. Note that the heat generation term on the right-hand side of Eq. (1) is not present in the high thermal conductivity pathways, as only the k_0-material generates heat.

The objective is to minimize the thermal resistance of the element, which translates in minimizing the hot spot tem-

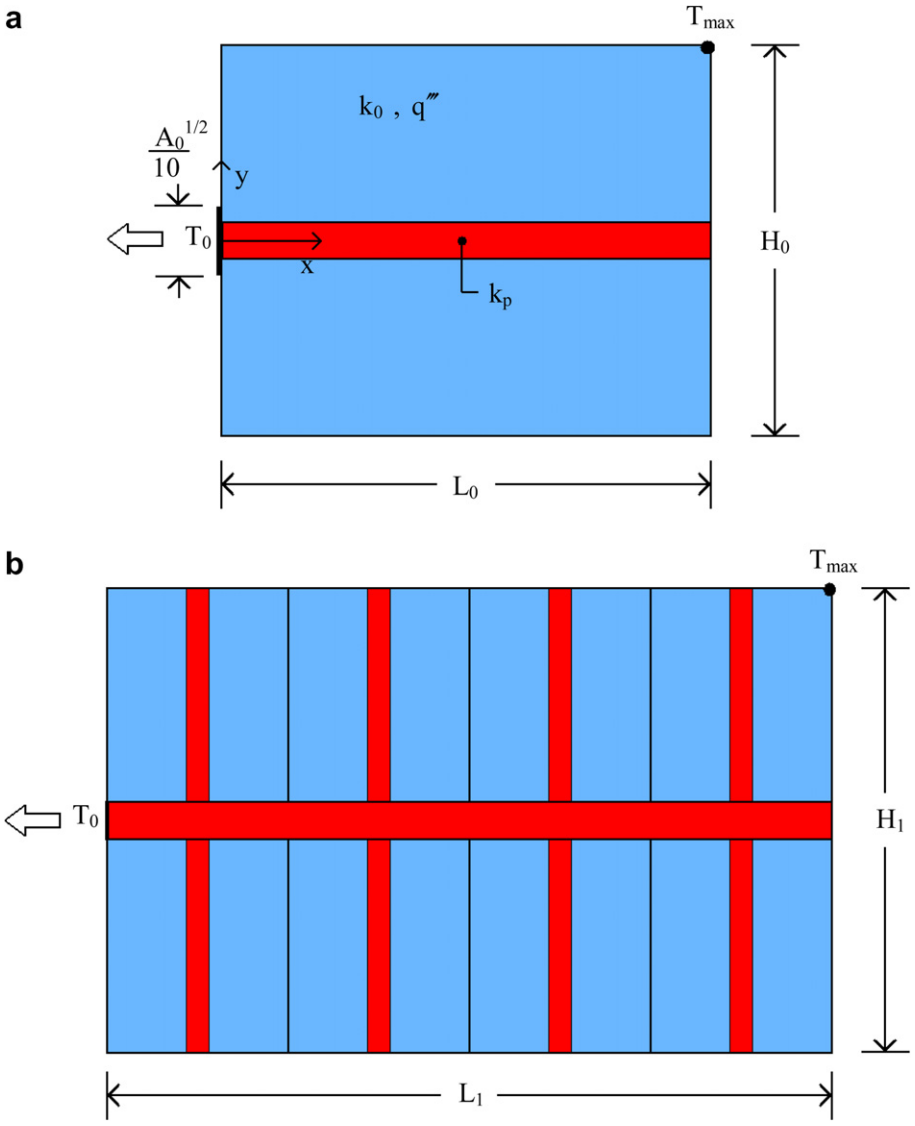

Fig. 1. The generation of optimal architectures with the constructal approach. (a) Elemental area, and (b) first construct.

perature of the area, $\widetilde{T}_{max}$. The hot spot temperature is the maximum temperature that is reached in the system, i.e., the weakest point of the design where thermal failure is most likely to occur. To achieve low hot spot temperature, the overall shape of the domain and the way that the high thermal conductivity is distributed will be varied. In other words, we want to generate the best composite architecture. In this paper, we consider that the size of the low temperature reservoir in contact with the system is fixed to 10% of $A^{1/2}$, see Fig. 1.

3. Numerical solving of the temperature profile

As mentioned previously, we consider in this paper an evolutionary optimization method for generating optimal configurations for the problem described in Section 2. The implementation of the optimization procedure requires a program for determining the temperature profile given the topology of the system. The program that we used for solving Eq. (1) is based on the finite volume (FV) method.

In order for the system to morph itself, i.e., to change its shape, we generate a computational domain (grid) 4 times larger than the actual dimensions of the system, so that during the evolution, the system will not be affected by the boundaries. The length of the domain is twice as large as its height. The grid is uniform with $\Delta\tilde{x} = \Delta\tilde{y}$, i.e., the length and height of each control volume has the same value for the entire domain. There are three types of control volumes in this mesh: (i) the heat-generating cells, with a dimensionless conductivity of 1; (ii) the high thermal conductivity cells ($k_p/k_0 \gg 1$) without heat generation; and (iii) the void cells (i.e., conductivity and heat generation set to zero). The void cells are present for the sole purpose of letting the system morph; they do not conduct nor generate heat. During the optimization, the non-void cells will

Table 1
Comparison between the results obtained with our code and the results presented in Ref. [4], with $H_0/L_0 = 1$

$\tilde{k}$	$\widetilde{T}_{max}$ (FE, Ref. [4])	$\widetilde{T}_{max}$ (FD, Ref. [4])	$\widetilde{T}_{max}$
300	0.126350	0.125519	0.126352
100	0.152859	0.151651	0.152865
10	0.408141	0.405452	0.408423

be able to move to void cell, and vice versa, similarly to pawns on a chessboards. Note that Eq. (1) is solved only in the non-void control volumes.

With a given distribution of cells, Eq. (1) is solved numerically with a finite volume (FV) code [18]. The equation is integrated on each control volume of the mesh, and effective thermal conductivities at the cell edges (faces) are extrapolated with harmonic means, see Ref. [18]. The integration results in a set of algebraic equations of the form $AT = b$, that can be solved with a standard line-by-line TDMA approach. For a given material distribution, convergence is declared when the hot spot temperature varies in value by less then 0.5% as the norm of the residual $\|AT - b\|/\|b\|$ dropped by one order of magnitude. More stringent convergence criteria were tested and did not change significantly the temperature profiles.

The code has been validated with a documented problem for which the geometry is similar to that shown in Fig. 1a. The hot spot temperature $\widetilde{T}_{max}$ obtained with our program are presented in Table 1, and compared with the results presented in [4], for $H_0/L_0 = 1$ and different values of k_p/k_0 with a 60×60 mesh. Note that, as in Ref. [4], $\widetilde{T}_{max}$ is defined as the maximum value of the temperature in the domain. The agreement can be considered very good as maximal discrepancy is smaller than 1%.

4. Evolutionary algorithm

The finite volume program described above has been coupled with an optimization algorithm for minimizing the thermal resistance of the composite structures investigated. The main steps of the optimization algorithm are summarized in Fig. 2. An initial distribution of materials is generated randomly. Invoking symmetry, only half of the domain is represented. In other words, the x-axis is considered as an axis of symmetry. Therefore, the heat sink sits on the bottom portion of the left-hand side numerical boundary (e.g., Fig. 3). An example of such an initial topology is depicted in Fig. 3a. Note that the x- and y-axis are the same as in Fig. 1a. Darker cells (in red in the color version of the paper[1]) represent the conductive material, and lighter (blue) cells, the heat-generating material. The initial distribution contains predetermined amount of heat-generating, conductive and void cells. We required that the non-void cells touch each other to avoid bundles of heat-generating cells disconnected from the heat sink. The temperature profile is then solved on the initial domain with the procedure described in the previous section (Section 3). An example of an initial temperature profile is shown in Fig. 3b.

Based on the temperature profile in the initial design, a certain number of cells are displaced (repositioned) with the objective of minimizing the hot spot temperature. In this paper, we considered two types of displacements:

(i) Swapping a void cell and a heat-generating cell.
(ii) Swapping a heat-generating cell and a conductive cell.

Note that during a move, no cell is created or eliminated as a volume constraint has been invoked. Cells are just repositioned.

There are several ways of selecting which cells to move [11–15]. Cell moving criteria could be based on the local temperature or heat flux information, or on more refined sensitivity analyses [11–15,19]. The former criteria (i.e., temperature or heat flux information) are faster to compute, but somewhat less precise, while the latter (i.e., sensitivity analysis) offer a better precision at the cost of more important computational time. Here, for the first type of moves (i.e., void-heat generating cells switch), the selection criteria used is based on the temperature information. The hot spot of the domain is identified. Then, we search for a void site in contact with the periphery for accepting the hot spot cell. The optimal site is the one for which the touching non-void cells have the lowest temperature. Finally, the swapping is performed: the identified void cell becomes a heat-generating cell, and the hot spot cell becomes a void cell.

The second type of moves (i.e., heat generating-conductive cells switch) is based on the local heat flux information. We calculated the local heat flux at the center of cells. Each component (x, y) of the local heat flux is determined by using adjacent cells temperature along with the discretized Fourier law. The norm of the heat flux vector is estimated in the high thermal conductivity cells. The cell with the smallest heat flux is identified. We ought to find a site where this conductive cell will contribute more efficiently to the heat removal. This site is located by finding the heat-generating cell with the largest heat flux. Then the switching of the low heat flux conductive cell and the large heat flux heat-generating cell is performed.

A comparison of the results obtained with different displacement criteria is presented in Table 2. We tested other combinations of criteria for moving cells, and the one that we presented above was the best in all the cases that we studied (e.g., second line in Table 2). The results were obtained with the same initial topology.

When the moves are completed, Eq. (1) is solved again with the program described above on the new topology in order to update the temperature profile (Fig. 2). This new topology is similar to the one of the previous iteration,

[1] For interpretation of color in Fig. 1, the reader is referred to the web version of this article.

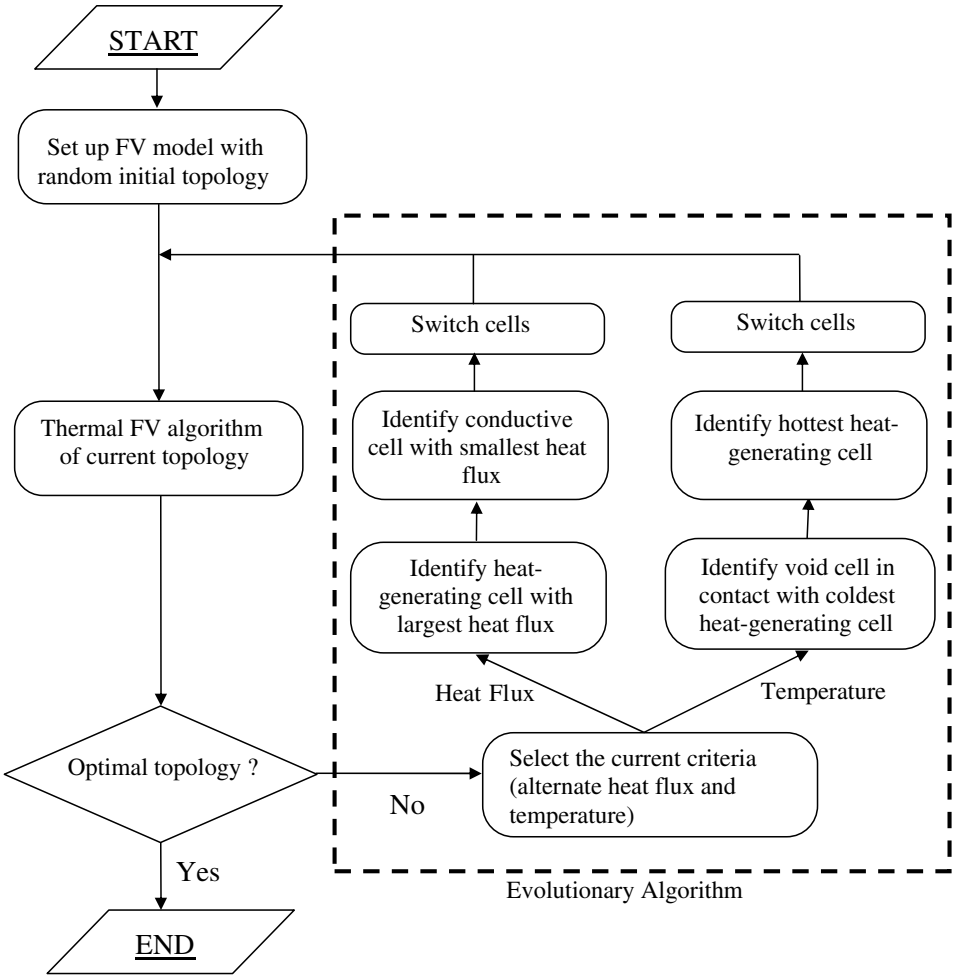

Fig. 2. The main steps of the optimization procedure.

as only one set of cell displacements is performed at a time, and therefore, given the temperature profile of the previous iteration as an initial guess for solving $\widetilde{T}$ on the new topology leads to a relatively rapid determination of $\widetilde{T}_{\max}$ on the new topology. The procedure (i.e., moving cells, calculating $\widetilde{T}$ on the new topology) is repeated until the hot spot temperature $\widetilde{T}_{\max}$ stops to evolve. In this paper, the optimization procedure is terminated when the total number of cell displacements performed from the beginning exceeds two thirds of the total number of non-void cells, as more displacements did not yield significant $\widetilde{T}_{\max}$ decrease. Fig. 3c and d shows an example of a typical final design with the corresponding temperature field, as obtained by the procedure described above. The color map (scale) in Fig. 3d in the online version of this paper is the same as in Fig. 3b, which explain why it appears mostly blue. In that case ($\tilde{k} = 10$ and $\phi = 0.2$), the hot spot temperature dropped by a factor 4.36 between the initial and final design. Video 1 in the online version of this article shows the evolution of the system as the optimization is performed.

Note that in several papers [13–16], only small fractions of cell constituents are displaced or removed step-by-step, generally based on a sensitivity analysis. At the end of the procedure, the optimal fraction of material in each cell is found. However, in reality, when each cell can only be either filled or empty, a post-treatment is required to extract the final topology from the domain with continuously varying material fractions. Here, the topology changes are discrete, not continuous. Therefore, no post-treatment is required.

Several mesh densities have been tested. There are two "types" of mesh independence studies related to this work: (i) for a given topology (i.e., materials distribution), the mesh can be refined until further grid doubling results in negligible changes in terms of the hot spot temperature, (ii) for a simulation with a given $\tilde{k}$ and ϕ, the total number of cells can affect the final topology achieved by the evolutionary algorithm. For instance, simulations with many small cells might allow thin branches to grow, which would not be possible with fewer and larger cells. Mesh size independence of type (i) was verified for each final topology, by doubling the mesh density in the final topology design until $\widetilde{T}_{\max}$ decreases by less than 1%. As for the point (ii) abovementioned, we reported in Fig. 4 the minimized hot spot temperature achieved for several mesh densities of initial random designs. Each point on that figure corresponds to the result of a full optimization. For a given mesh density, we obtained different values of $\widetilde{T}_{\max}$ with each run as the

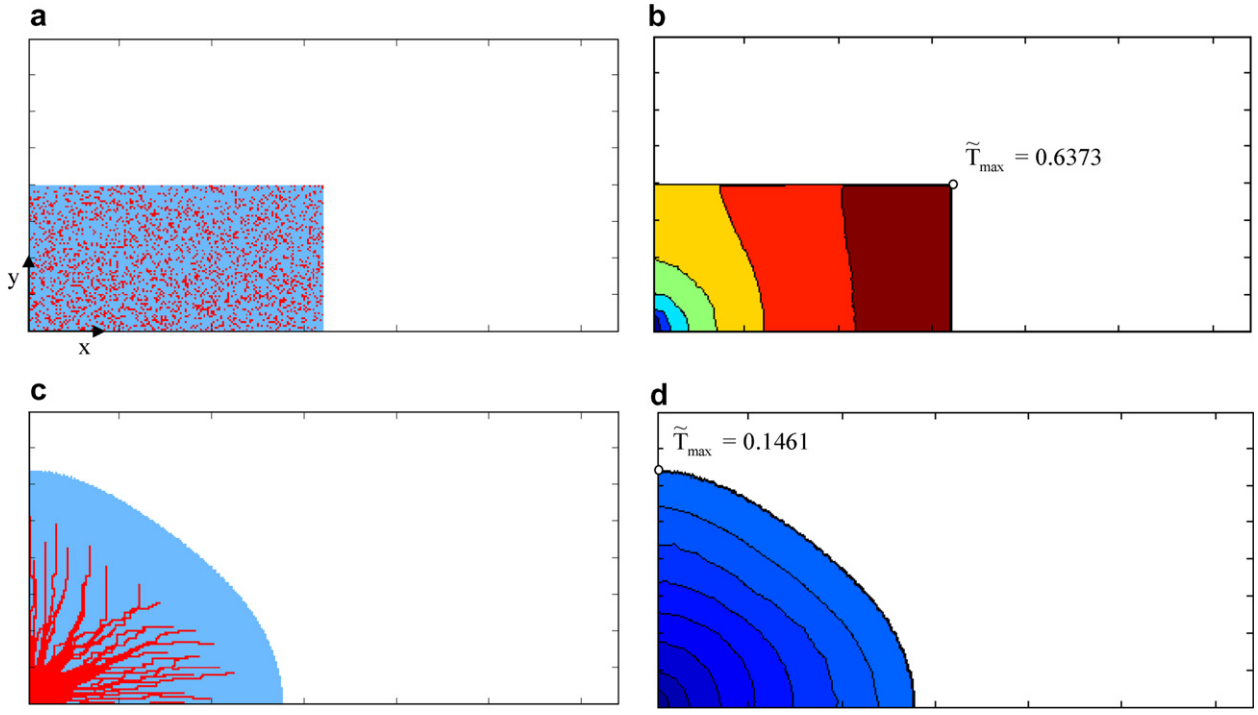

Fig. 3. Example of an optimization run with $\tilde{k} = 10$, and $\phi = 0.2$. (a) Initial random topology, (b) temperature field in the initial topology, (c) optimized topology, and (d) temperature field in the optimized structure.

Table 2
Comparison between the minimal hot spot temperatures achieved with different cell displacement criteria

Displacement criterion for heat-generating and void cells switch	Displacement criterion for high conductivity and heat-generating cells switch	$\widetilde{T}_{max,m}$
Temperature	Temperature	2.2866×10^{-1}
Temperature	Heat flux	$\mathbf{5.0964 \times 10^{-2}}$
Heat flux	Temperature	3.6824×10^{-1}
Heat flux	Heat flux	6.4044×10^{-2}

initial materials distribution was randomly selected. Note that the $\widetilde{T}_{max}$-values are extracted from the temperature fields brought to mesh independence, i.e., when $\widetilde{T}_{max}$ change is less than 1% when doubling grid of the final design. As expected, Fig. 4 shows that larger numbers of cells (i.e., finer meshes) yield to better performances due to greater numbers of possible topologies. However, a plateau is eventually reached which means that at some point, more freedom to morph is not useful in terms of thermal performance. Most importantly, finer meshes offer a better repeatability. For instance, the standard deviation with respect to the average value of the $\widetilde{T}_{max,m}$ achieved with a 10×20 mesh is 13.9% while the standard deviation is only 2.4% for a 80×160 mesh.

For most results presented in this paper, optimization grids with 80×160 cells were used as further grid doubling resulted in negligible hot spot temperature reduction. The optimization runs were performed with a 80×160 mesh, and the final value of $\widetilde{T}_{max}$ was determined with mesh independence as defined above.

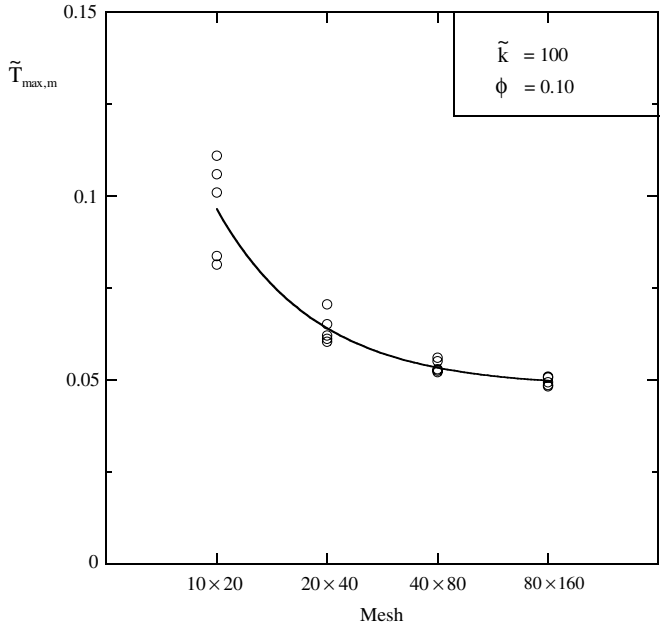

Fig. 4. The influence of the mesh density on the thermal performance of the optimized topology.

5. Optimization results with the evolutionary algorithm

The initial design from which the evolutionary algorithm is initiated has an impact on the final "optimal" design. In order to avoid creating any bias for the output designs, we began the optimization runs with randomly distributed

materials, as mentioned previously. With that approach, each run of the program can potentially lead to a different "optimum" because the initial (random) design can vary. To study the repeatability of the results (i.e., optimal design, minimal hot spot temperature), we performed three runs with the same parameter settings ($\tilde{k} = 100$ and $\phi = 0.1$), the only difference between the runs being the initial random distribution of materials. The results are presented in Fig. 5. As expected, the differences in the initial random topologies resulted in different final topologies. Despite "visual" discrepancies, all the topologies share a certain number of features (e.g., branching complexity of the conductive pathways, external shape). More importantly, the variations of the minimized hot spot temperature between the different runs are small (less than 3%), which reinforces the idea that tree-shaped network are robust [4]. The three designs proposed in Fig. 5 are thus acceptable nearly-optimal designs.

The position of the hot spot (indicated by a small circle) varies significantly between the runs, but it is located on the outer rim of the heat-generating system in each case.

The effect of the thermal conductivity ratio is presented in Fig. 6, where the optimal topology for three $\tilde{k}$-values are depicted ($\tilde{k} = 10, 100, 1000$) at constant ϕ. As the thermal conductivity is increased, the conductive network evolves from fewer, thicker branches to a network with several narrow blades. Loops in the conductive network are generated when $\tilde{k}$ is sufficiently large. The external shape of the system is also sensible to $\tilde{k}$. When $\tilde{k} = 10$, the external shape is especially smooth. For larger values of the thermal conductivity, finger-shaped protrusions grow on the outer rim. The minimized hot spot temperature diminishes when the conductivity increases, reaching values of 2.192×10^{-1}, 4.833×10^{-2}, and 9.477×10^{-3} for $\tilde{k}$-values of 10, 100,

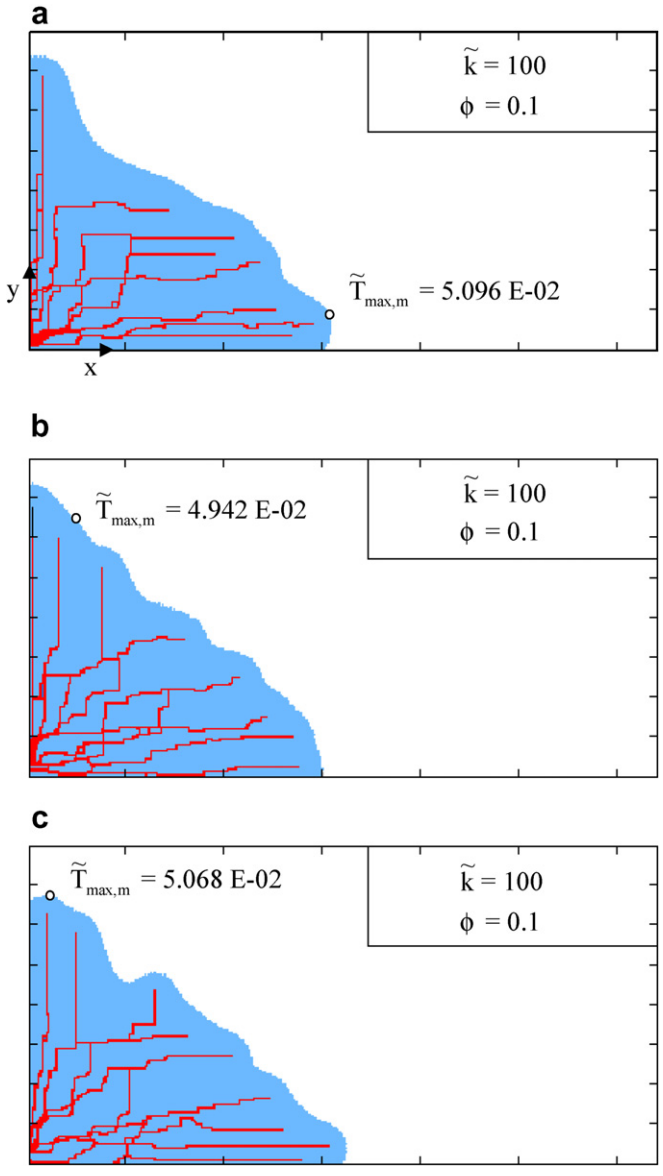

Fig. 5. The optimal topology obtained with three simulations considering the same parameters ($\phi = 0.1$ and $\tilde{k} = 100$).

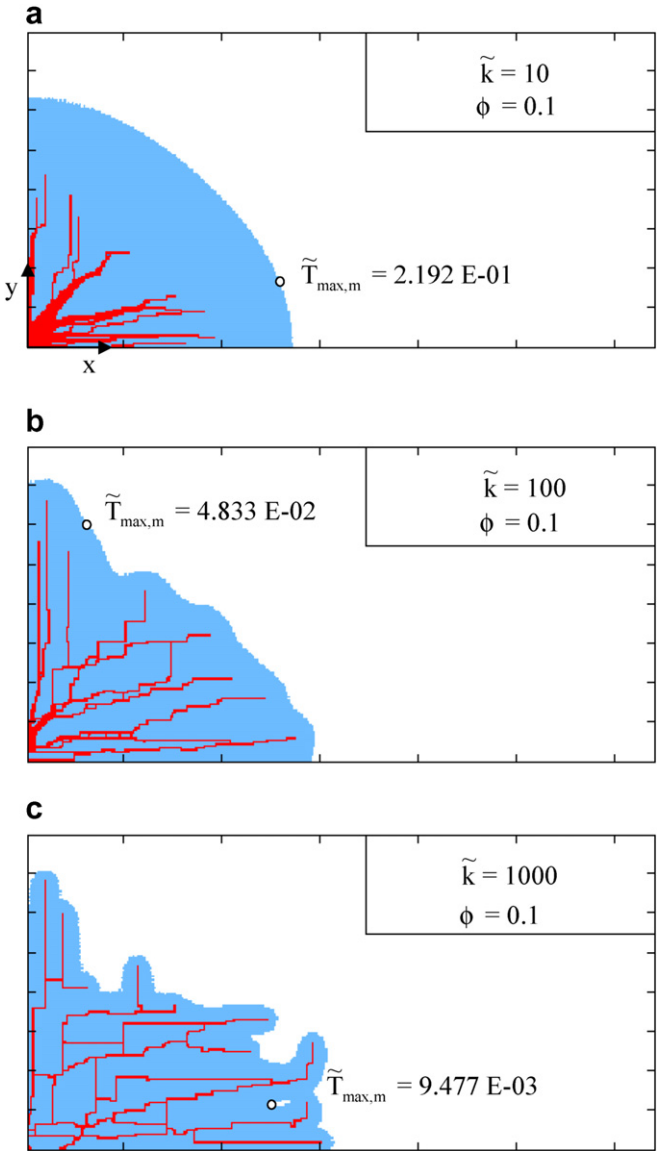

Fig. 6. The effect of the thermal conductivity on the optimal topology and hot spot temperature with $\phi = 0.1$, and (a) $\tilde{k} = 10$, (b) $\tilde{k} = 100$, and (c) $\tilde{k} = 1000$.

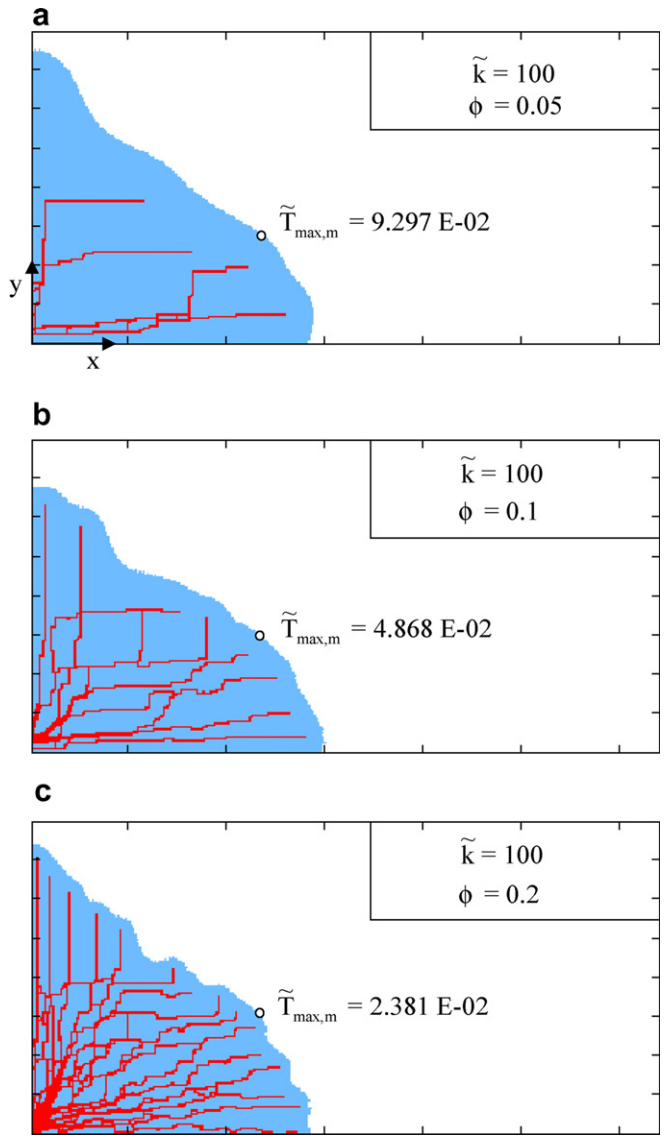

Fig. 7. The effect of the amount of high thermal conductivity material on the optimal topology and hot spot temperature with $\tilde{k} = 100$, and (a) $\phi = 0.05$, (b) $\phi = 0.1$, and (c) $\phi = 0.2$.

and 1000, respectively. Roughly speaking, the temperature reduces by ~80% when $\tilde{k}$ is multiplied by 10.

Fig. 7 reveals the effect of the amount of high thermal conductivity material on the final optimal topology, with different ϕ-values. The external shape of the system is comparable in each case. However, the conductive network is significantly different in each case. The number of branches and loops augments with ϕ. The minimal hot spot temperature achieved with ϕ-values of 0.05, 0.1, and 0.2 were 9.297×10^{-2}, 4.868×10^{-2}, and 2.381×10^{-2}, respectively. The hot spot temperature approximately doubles when ϕ is divided by a factor 2.

6. Constructal theory viewpoint

In this section, we recall briefly the principal outcomes of constructal theory for the generation of minimal thermal resistance composite architectures. Detailed results can be found elsewhere [2,3]. The objective of this section is to offer a basis for comparing the levels of performance, and the geometrical features of the systems optimized with the evolutionary procedure (see Section 7). The procedures themselves will be compared as well. The constructal approach begins with an elemental area, Fig. 1a, consisting of a high thermal conductivity blade within a rectangular heat-generating area. Due to the two constraints invoked previously (i.e., fixed area $A_0 = H_0 L_0$, fixed amount of high thermal conductivity material ϕ_0), there is only one design variables left to minimize the hot spot temperature. The analytical expression of the temperature drop $(T_{\max} - T_0)$ can be minimized with respect to H_0/L_0 leading to [2,3]:

$$\left(\frac{H_0}{L_0}\right)_{\text{opt}} = 2(\tilde{k}\phi_0)^{-1/2},$$

$$\Delta\tilde{T}_{0,\text{m}} = \left(\frac{T_{\max,\text{m}} - T_0}{q''' A_0/k_0}\right)_0 = \frac{1}{2}(\tilde{k}\phi_0)^{-1/2} \tag{3}$$

where $\phi_0 = D_0/H_0$ is the ratio of A_0 occupied by the blade.

Once the elemental area has been optimized, it is possible to assemble several of them along a new blade to form a first construct of area A_1, Fig. 1b, which can be optimized with respect to n_1 (number of elemental areas in the first construct), and ϕ_0/ϕ_1 (ratio of the high thermal conductivity material in the elemental structures). The optimization results in [3]:

$$\left(\frac{H_1}{L_1}\right)_{\text{opt}} = 2, \quad \Delta\tilde{T}_{1,\text{m}} = \left(\frac{T_{\max,\text{m}} - T_0}{q''' A_1/k_0}\right)_1 = (\tilde{k}\phi_1)^{-1} \tag{4}$$

$$\phi_{0,\text{opt}} = \frac{1}{2}\phi_1, \quad n_{1,\text{opt}} = (\tilde{k}\phi_1/2)^{1/2} \tag{5}$$

The same procedure can be pursued to achieve higher levels of construct. A multiscale tree-shaped network of high-conductivity material, optimized at each level of construct, emerges from the procedure. This structure is an optimization result, not an assumption. The optimization procedure is in the direction from the smallest to the largest elements [3].

We can compare on the basis of a constant area A and amount of conductive material, ϕ, the performance of the different construct topologies [19]. For example, the hot spot temperature ratio of the first construct to that of the elemental surface is $2(\tilde{k}\phi)^{-1/2}$. In other words, the elemental construct is better when $\tilde{k}\phi \lesssim 4$, and the first construct when $\tilde{k}\phi \gtrsim 4$. Furthermore, the number of branches, Eq. (5), increases with $\tilde{k}\phi$. Therefore, as the quantity $\tilde{k}\phi$ increases in a fixed area, one should expect optimal structures with more branches, and higher "levels of complexity". In the next section, we compare our optimization results with the ones described in this section.

7. Comparison with constructal heat trees and complexity assessment

Guided by the analysis presented in the previous section and in Ref. [3], we suspected that the separate influence of $\tilde{k}$

and ϕ on $\widetilde{T}_{\max,m}$ as obtained by the evolutionary algorithm could be expressed in terms of a single parameter, which is the product $\tilde{k}\phi$. Therefore, we plotted in Fig. 8 the minimized hot spot temperature as a function of the quantity $\tilde{k}\phi$. Each point on that figure is the result of a full optimization. Several combinations of $\tilde{k}$ and ϕ leading to the same product $\tilde{k}\phi$ were considered. The results seem to confirm that $\tilde{k}\phi$ is a governing quantity for determining the level of performance of heat trees, as most points fall onto the curve. For the sake of comparison, the value of $\tilde{T}_{\max,m}$ for the elementary and first level constructs from constructal theory [4] (Section 6) are also plotted in Fig. 8. The thermal resistances of the evolutionary optimized structures are somewhat smaller than the one predicted by constructal theory due to the larger number of design variables considered (more freedom to morph).

To conclude this exercise, we wanted to assess the "complexity" of the topologies that we obtained, and compare that complexity with the one predicted by constructal theory. Let $\widetilde{R}_i$ be the dimensionless distance between a conductive cell 'i' and the heat sink (located at the bottom of the left-hand side boundary in figures). In Fig. 9, we reported the average dimensionless distance $\overline{R} = (\sum_{i=1}^{N} \widetilde{R}_i)/N$ from the origin of the conductive cells. The average distance is a measure of the dispersion of the conductive cells within the heat-generating area. As $\tilde{k}\phi$ increases, so does the average distance from the center. In other words, the high thermal conductivity pathways span more widely for large $\tilde{k}\phi$-values. This is also the case for the elemental and first level construct of constructal theory, as depicted in Fig. 9.

For each heat-generating cell, the minimal distance from the conductive network has been calculated. Thus, let $\widetilde{D}_i$ be the distance between a heat-generating cell 'i' and its nearest conductive cell. In order to measure how uniformly distributed the conductive material is, the average of these minimal distances to the high-conductivity pathways $\overline{D} = (\sum_{i=1}^{N} \widetilde{D}_i)/N$ is determined, and reported in Fig. 10 as a function of $\tilde{k}\phi$. It is globally a decreasing function of $\tilde{k}\phi$, similarly to the constructal trees.

Fractal dimension d_f of the 2D shape defined by the heat-generating material were calculated using the average

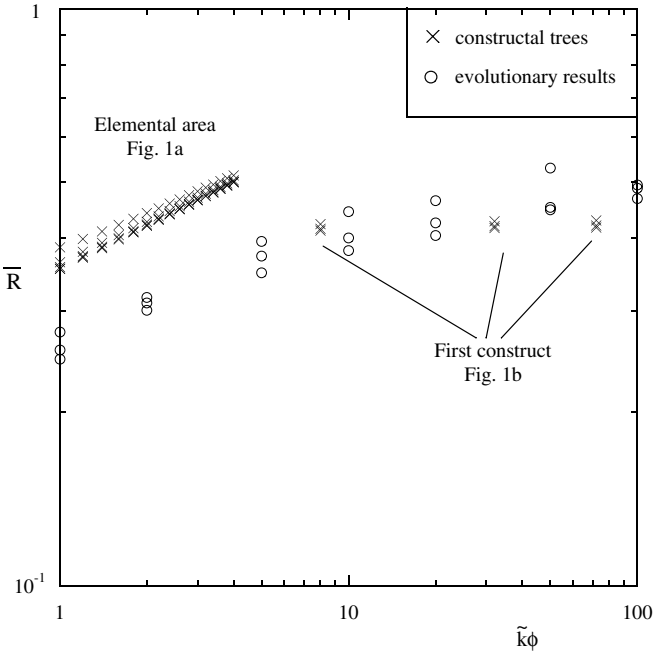

Fig. 9. The average distance $\overline{R}$ from the origin of the conductive cells as a function of $\tilde{k}\phi$.

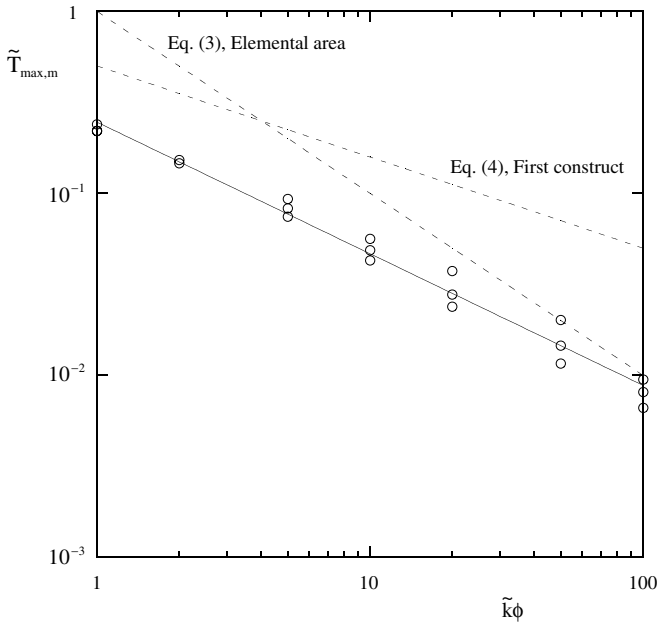

Fig. 8. The minimized hot spot temperature as a function of the parameter $\tilde{k}\phi$.

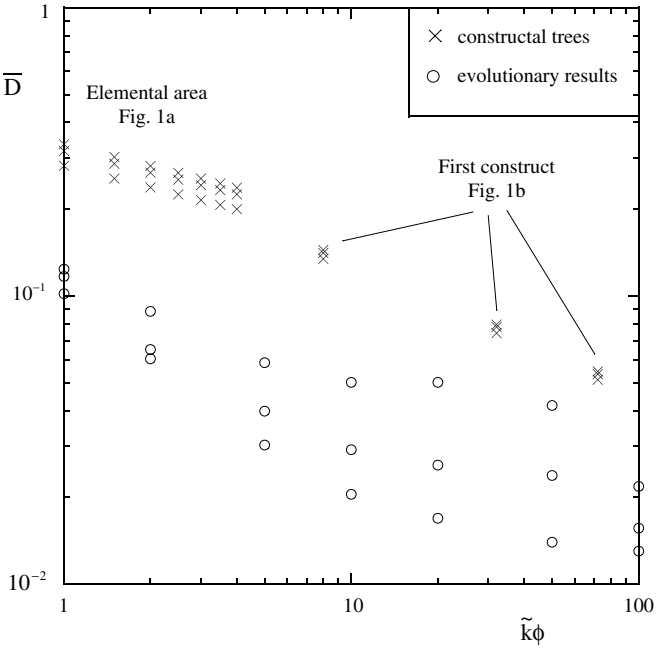

Fig. 10. The average of the minimal distance $\overline{D}$ between the heat-generating cells and the conductive network as a function of $\tilde{k}\phi$.

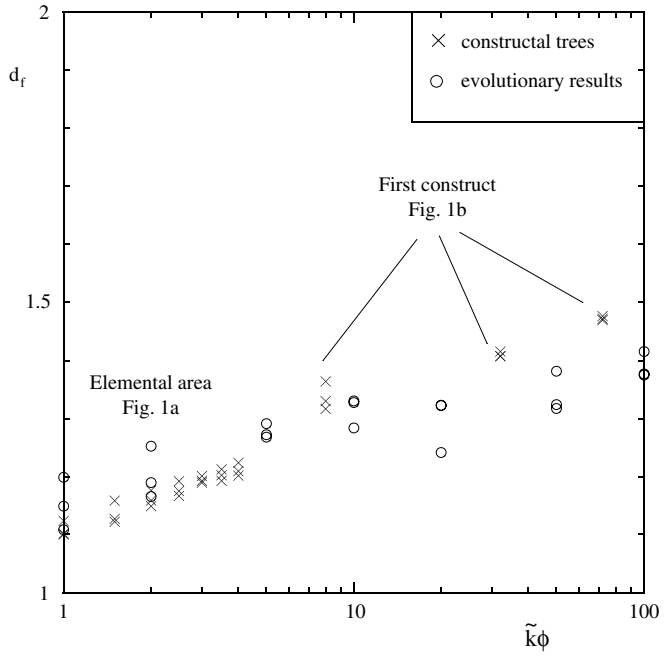

Fig. 11. The fractal dimension (d_f) of the generated shapes of heat trees compared to the fractal dimension of the constructal trees, as a function of $\tilde{k}\phi$.

mass dimension approach. It is defined as the slope in a log–log diagram of the counted average distance versus precision (see appendix in Ref. [20] for the detailed algorithm). Results are presented in Fig. 11. The fractal dimensions (d_f) increases with $\tilde{k}\phi$. For the sake of comparison, the fractal dimensions of constructal heat trees are also reported in Fig. 11. It is worth to indicate that the fractal dimensions in Fig. 11 are deduced, not assumed. They are results, not assumptions. This differentiates this work from others (e.g., [21]) in which fractal dimensions are a priori model inputs, rather than knowledge deduced from post-treatment.

In a recent work about the cooling of a heat-generating disk-shaped area with a heat sink located at its center, it was shown that distinct optimal conductive structures appear as different constraints are applied [22]. These optimal conductive network configurations are: (i) radial blades; (ii) tree-shaped branches; (iii) looping branches, all of these making contact with the central heat sink and "vascularizing" the area toward the periphery. Although the general morphing allowed by the evolutionary algorithm used here did not provide as idealized geometries, each topological optimization has led to architectures that match with the three basic geometries mentioned above (see Figs. 6 and 7).

In our simulations, for $\tilde{k}\phi \lesssim 4$, the characteristic optimal structures are with radial blades that extend from the heat sink, decreasing in thickness with radial distance, and expanding farther in the heat generating material as the $\tilde{k}\phi$-constraint increases. The constructal theory predicts that one radial blades leads to smaller thermal resistance in that range of $\tilde{k}\phi$, which is consistent with our observations.

For $4 \lesssim \tilde{k}\phi \lesssim 50$, our optimized topologies revealed branches with many levels of bifurcations (tree-shaped geometrical features). Constructal theory predicts increasing number of branches as $\tilde{k}\phi$ increases in that range, Eq. (5). Finally, for $\tilde{k}\phi \gtrsim 50$, most of the high-conductivity branches are part of a looping network that expands through the heat-generating material. Loops are often associated with system robustness [3,22].

8. Conclusions

In this paper, we addressed the problem of optimizing material allocation for maximal cooling in conduction. An evolutionary strategy was implemented for morphing an initial architecture toward an optimal design. Simple temperature and heat flux criteria were used to locate cells to move, and significant hot spot temperature diminutions were observed. Further research could combine local and global evolutionary optimizations by dividing the domain into sub-systems.

An objective of the paper was to compare the constructal and evolutionary procedures. In both cases, the geometrical features of the final designs are not assumed, they are result of optimization. This differentiates these approaches from a priori (assumed) fractal-like designs. Another similarity between both approaches is that they follow a "time" arrow: our evolutionary procedure displaced small building blocks in a step-by-step fashion, and constructal design optimizes "from the smallest to the largest". The evolutionary algorithm could also be used to optimize "growing" structures simply by adding in an optimal way, and step-by-step, new cells to an initial smaller design.

The geometrical features of the optimized structures have been assessed with the help of different factors, and appeared to vary significantly with the parameter $\tilde{k}\phi$. Our evolutionary algorithm showed that the optimal high conductive architectures progress from few radial blades, to tree-shaped branches and ends with looping networks as the $\tilde{k}\phi$-constraint increases. These three fundamental geometries were also exhibited in constructal theory related papers about heat trees [3–10,22] and even fluid distribution networks [23–25]. Further comparative morphing studies could involve convection heat transfer structures [26].

Acknowledgements

L. Gosselin's work was supported by the *Fonds québécois de recherche sur la nature et les technologies* (FQRNT) of the Province of Québec, via the New Researchers Start-Up Program.

Appendix A. Supplementary data

Supplementary data associated with this article can be found, in the online version, at doi:10.1016/j.ijheatmasstransfer.2006.12.020.

References

[1] A.E. Bergles, Evolution of cooling technology for electrical, electronic, and microelectronic equipment, IEEE Trans. Compon. Pack. Technol. 26 (1) (2003) 6–15.

[2] A. Bejan, Constructal-theory network of conducting paths for cooling a heat generating volume, Int. J. Heat Mass Transfer 40 (4) (1997) 799–816.

[3] A. Bejan, Shape and Structure: From Engineering to Nature, Cambridge University Press, Cambridge, UK, 2000.

[4] G.A. Ledezma, A. Bejan, M.R. Errera, Constructal tree networks for heat transfer, J. Appl. Phys. 82 (1) (1997) 89–100.

[5] M. Almogbel, A. Bejan, Conduction trees with spacings at the tips, Int. J. Heat Mass Transfer 42 (20) (1999) 3739–3756.

[6] M. Neagu, A. Bejan, Three-dimensional tree constructs of constant thermal resistance, J. Appl. Phys. 86 (12) (1999) 7105–7115.

[7] L. Ghodoossi, N. Egrican, Conductive cooling of triangular shaped electronics using constructal theory, Energy Convers. Manage. 45 (6) (2004) 811–828.

[8] L.A.O. Rocha, S. Lorente, A. Bejan, Constructal design for cooling a disc-shaped area by conduction, Int. J. Heat Mass Transfer 45 (8) (2002) 1643–1652.

[9] A.K. da Silva, C. Vasile, A. Bejan, Disc cooled with high-conductivity inserts that extend inward from the perimeter, Int. J. Heat Mass Transfer 47 (19–20) (2004) 4257–4263.

[10] L. Gosselin, A. Bejan, Constructal heat trees at micro and nanoscales, J. Appl. Phys. 96 (10) (2004) 5852–5859.

[11] Q. Li, G.P. Steven, O.M. Querin, Y.M. Xie, Shape and topology design for heat conduction by evolutionary structural optimization, Int. J. Heat Mass Transfer 42 (17) (1999) 3361–3371.

[12] G.P. Steven, Q. Li, Y.M. Xie, Evolutionary topology and shape design for general physical field problem, Comput. Mech. 26 (2) (2000) 129–139.

[13] Q. Li, G.P. Steven, Y.M. Xie, O.M. Querin, Evolutionary topology optimization for temperature reduction of heat conducting fields, Int. J. Heat Mass Transfer 47 (23) (2004) 5071–5083.

[14] A. Gersborg-Hansen, M.P. Bendsøe, O. Sigmund, Topology optimization of heat conduction problems using the finite volume method, Struct. Multidiscip. Optim. 31 (4) (2006) 251–259.

[15] C.-H. Cheng, H.-H. Lin, W. Aung, Optimal shape design for packaging containing heating elements by inverse heat transfer method, Heat Mass Transfer 39 (8–9) (2003) 687–692.

[16] A.A. Novotny, R.A. Feijóo, E. Taroco, C. Padra, Topological sensitivity analysis, Comput. Methods Appl. Mech. Eng. 192 (7-8) (2003) 803–829.

[17] A.-H. Wang, X.-G. Liang, J.-X. Ren, Constructal enhancement of heat conduction with phase change, Int. J. Thermophys. 27 (1) (2006) 126–138.

[18] J.C. Tannehill, D.A. Anderson, R.H. Pletcher, Computational Fluid Mechanics and Heat Transfer, second ed., Taylor&Francis, 1997.

[19] A. Bejan, N. Dan, Two constructal routes to minimal heat flow resistance via greater internal complexity, J. Heat Transfer 121 (1999) 6–14.

[20] W. Borkowski, Fractal dimension based features are useful descriptor of leaf complexity and shape, Can. J. Forest Res. 29 (9) (1999) 1301–1310.

[21] P. Xu, B. Yu, M. Yun, M. Zou, Heat conduction in fractal tree-like branched network, Int. J. Heat Mass Transfer 49 (2006) 3746–3751.

[22] L.A.O. Rocha, S. Lorente, A. Bejan, Conduction tree networks with loops for cooling a heat generating volume, Int. J. Heat Mass Transfer 49 (15–16) (2006) 2626–2635.

[23] L. Gosselin, A. Bejan, Tree networks for minimal pumping power, Int. J. Therm. Sci. 44 (1) (2005) 53–63.

[24] W. Wechsatol, S. Lorente, A. Bejan, Optimal tree-shaped networks for fluid flow in a disc-shaped body, Int. J. Heat Mass Transfer 45 (25) (2002) 4911–4924.

[25] W. Wechsatol, S. Lorente, A. Bejan, Tree-shaped networks with loops, Int. J. Heat Mass Transfer 48 (3–4) (2005) 573–583.

[26] A.K. da Silva, A. Bejan, S. Lorente, Maximal heat transfer density in vertical morphing channels with natural convection, Numer. Heat Transfer, Part A: Appl. 45 (2) (2004) 135–152.